Ultralight Weight Optical Systems using Nano-Layered Synthesized Materials

Natalie Clark
NASA Langley Research Center
Hampton Virginia, 23681; 757-864-5662
Natalie.clark-1@nasa.gov

James Breckinridge
University of Arizona, College of Optical Sciences
1630 E. University Blvd, Tucson AZ 85721; 626-318-0339
jbreckin@earthlink.com

ABSTRACT

Optical imaging is important for many NASA science missions. Even though complex optical systems have advanced, the optics, based on conventional glass and mirrors, require components that are thick, heavy and expensive. As the need for higher performance expands, glass and mirrors are fast approaching the point where they will be too large, heavy and costly for spacecraft, especially small satellite systems. NASA Langley Research Center is developing a wide range of novel nano-layered synthesized materials that enable the development and fabrication of ultralight weight optical device systems that enable many NASA missions to collect science data imagery using small satellites. In addition to significantly reducing weight, the nano-layered synthesized materials offer advantages in performance, size, and cost.

INTRODUCTION

Optical imaging is important for many NASA science missions. Even though complex optical systems have advanced, the optics, based on conventional glass and mirrors, require components that are thick, heavy and expensive. As the need for higher performance expands, glass and mirrors are fast approaching the point where they will be too large, heavy and costly for spacecraft, especially small satellite systems. NASA Langley Research Center is developing a wide range of novel nano-layered synthesized materials that enable the development and fabrication of ultralight weight optical device systems that enable many NASA missions to collect science data imagery using small satellites. In addition to significantly reducing weight, the nano-layered synthesized materials offer advantages in performance, size, and cost.

In addition to a significant reduction in weight, nano-layer synthesized materials enable optical properties that no single material can match. The optical properties of conventional materials inherently depend on the wavelength of light. One advantage of synthesized nano-layered materials is that the wavelength dependence of the material can be held constant over a large spectral bandwidth. The synthesized nano-layered material can also be custom designed to provide a desired spectral response over desired bandwidths or a desired phase and polarization response. Another advantage of such materials is that they lend themselves to use as large thin diffraction telescope components in an optical imaging system. Diffraction inherently causes significant chromatic, polarization and wavefront aberrations. Consequently, diffractive optical elements are not typically used in large telescope systems, especially for broad band imaging applications. By using nano-layered synthesized materials, the diffractive optics are capable of diffraction-limited imaging over a large spectral bandwidth.

Designing optical devices and systems using nano-layered synthesized materials allows for unprecedented design flexibility. In this paper, a design methodology is presented along with performance analyses for specific small satellite applications. The paper will also present material fabrication considerations along with experimental results that characterize the imaging performance. The fabrication methods presented utilize rapid prototyping techniques that enable very low cost

custom and semi-custom fabrication, tailored to specific mission requirements. Particular NASA small satellite applications including helio-physics, exoplanet photometry and Guidance, Navigation and Control (GNC) will be presented along with experimental results characterizing overall system performance of the nano-layered materials.

NANO-LAYERED SYNTHESIZED MATERIALS

In general, it is not easy (and even impossible) to find materials that have all the properties needed for a particular application. Nano structured materials offer the ability to combine materials and structures to enable overall performance that no single material would be able to provide. Nanostructured materials such as nano-layered synthesized materials are currently of intense interest in modern materials research[1-3]. As discussed in this paper, the nano-layered synthesized materials are fabricated using optical fabrication techniques that are designed with different stacking sequences and layer thicknesses. The properties of fabricated nano-layered synthesized materials depend on their compositions and thicknesses. These can be demonstrated within the synthesis process by thickness control of each layer and interfacial light propagation between the nano-layers. Synthesized materials that stack layers of materials at the micro and nano scale offer a means of designing components to have the desired specifications.

DIFFRACTIVE TELESCOPE SYSTEM

One approach for constructing large light weight optical telescope systems is to use a diffractive Fresnel lens or mirror as the telescope objective. Conventional refractive (lens) or reflective (mirror) components require high precision optical tolerances that are difficult or even impossible to manufacture for a zero-g space environment. A Fresnel lens or mirror offers a way to use a flat diffractive component, thus eliminating the need for high precision 3D (out of plane) fabrication.

A schematic layout of a novel telescope system utilizing components fabricated in the LaRC advanced optics cleanroom facility is shown in Figure 1. Referring to the figure, the telescope objective is a light weight optical sieve consisting of millions of diffractive holes. The optical sieve telescope objective acts as a diffractive lens element focusing the light at the focal plane. The adaptive optics and fast steering mirror is able to focus the light, correct the wavefront aberration and facilitate tracking and beam steering of objects of interest. As discussed in this paper, the optical sieve is a spectrally dispersive element. The tunable filter enables the light to be spectrally filtered so that the image focused by the adaptive optics is all in focus. Depending on the design of the telescope, a diffractive optical element (DOE) is used to enable broad band imaging. The Inertial Measurement Unit (IMU) allows for the high bandwidth positioning of the telescope system to be relayed to the steering mirror to keep the objects of interest within the field of view and stabilized.

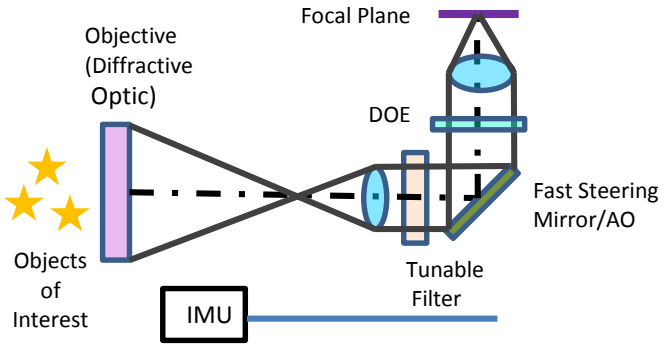

Figure 1. Concept layout of the Ultralight weight Diffractive Optical Telescope System.

Diffractive Telescope Objective

A photon sieve is based on a sparse aperture Fresnel zone plate[4-6]. It consists of concentric transparent and opaque. Figure 2 shows the layout of a photon sieve fabricated at Langley. The white holes in the layout are transparent and the black regions are opaque. Table 1 summarizes the relevant equations useful for designing a photo sieve.

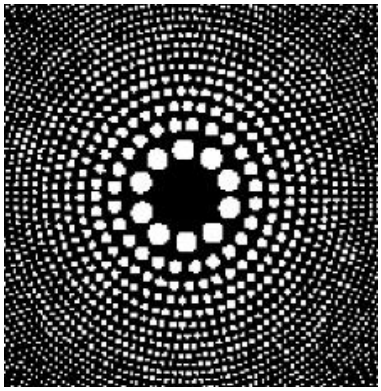

Figure 2. Optical Sieve layout.

Table 1: Telescope Optical Expressions

Optical Parameter	Mathematical Expression
Zone Radius	$r_n{}^2 = 2n\lambda f + n^2\lambda^2$
Zone Width	$w = \frac{\lambda f}{2r_n}$
Dispersion	$\Delta\lambda = \frac{2\lambda^2 f}{D^2}$
Resolution	$resolution = \frac{1.22\lambda}{D}$
Spot Size Δ	$\Delta = \frac{1.22\lambda f}{D}$
Depth of focus (DOF)	DOF = $\pm\frac{2\Delta^2}{\lambda}$
Bandpass $\Delta\lambda$	$\Delta\lambda = \frac{2\lambda^2 f}{D^2}$

Telescope Objective Design and Performance

Several photon sieves were designed and fabricated for remote sensing of the sun and stars. The photon sieve can characterized by three key parameters. Other optical properties can be inferred from these three parameters. Typically, an application has a specific mission in mind. For example, for a heliophysics application both the UV and visible light are of particular interest for imaging the sun. For the star tracker application, the visible spectrum is of interest. The number of Fresnel rings that can be fabricated is limited by the fabrication process. In the fabrication process one micron holes have been achieved near the diffraction limit of the UV photolithography light. The diameter is chosen to provide the desired spatial resolution. To facilitate the design process, the plots of focal length, depth of focus in Figures 3 and 4 are very useful.

The focal length of the telescope objective depends on the hole size. Figure 3 is a graph of the focal length in meters versus wavelength for particular hole sizes of 1, 2, 5 and 10 microns. The LaRC fabrication allows for a one micron resolution and hence the focal length for 656.28 nm (solar H-alpha line) is reduced by over a factor of 6.

The photon sieve is a diffractive element and it inherently suffers from dispersion that results in a focal length varying linearly with wavelength. The depth of focus is limited to a spectral bandwidth shown in Table 1 and graphically portrayed as a function of wavelength, focal length and fabrication hole sizes in Figure 4. The depth of focus does not depend on the aperture size of the telescope objective.The depth of focus is limited to a bandpass $\Delta\lambda$ shown in Table 1. It is possible to remove a significant amount of this dispersion by

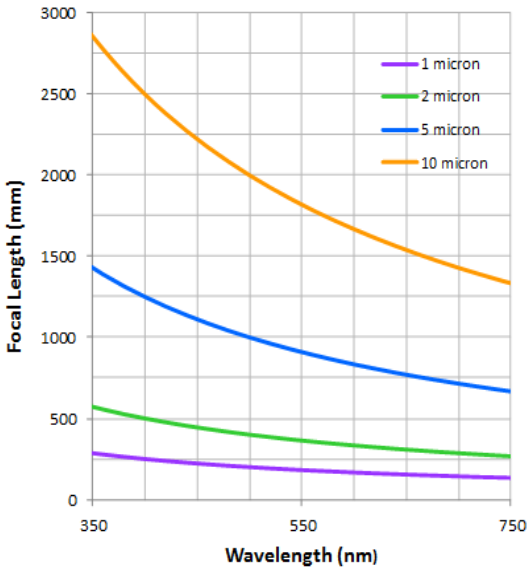

Figure 3. Optical Sieve plot of focal length versus wavelength.

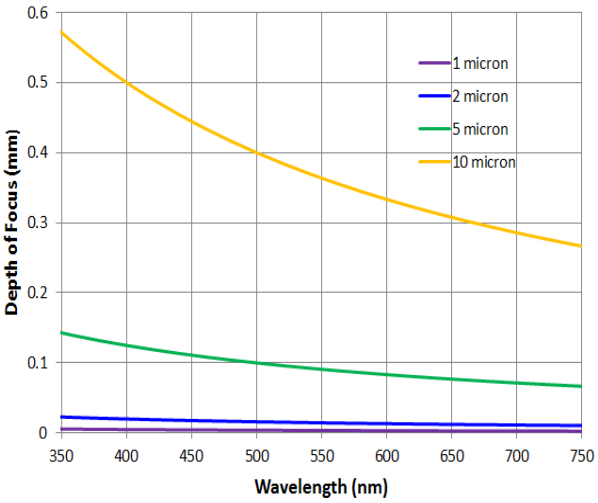

Figure 4. Depth of Focus of Optical Sieve.

using a secondary diffractive optical element (DOE) to increase the bandwidth to 40nm or more. As the F# becomes smaller the design constraints on the broadband correction become increasingly and perhaps prohibitively tight. Hence, the photon sieve, without any other components in the optical system, is better suited

to high resolution, narrowband imaging applications rather than having broadband applications.

Diffractive Telescope Objective Fabrication and Performance Evaluation

The optical sieve can be manufactured on thin ridged substrates or flexible membrane substrates. The diffractive telescope objective can also be fabricated to be reflective or transmissive. Figure 5 shows a schematic of the basic process used in the advanced optics laboratory to fabricate the micro- and nano-layer synthesized materials.

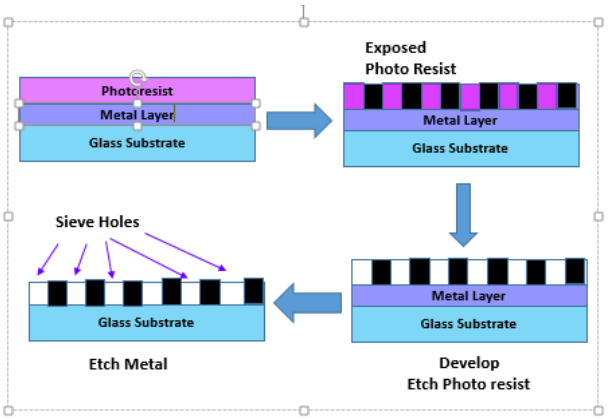

Figure 5. Schematic of the optical sieve fabrication process.

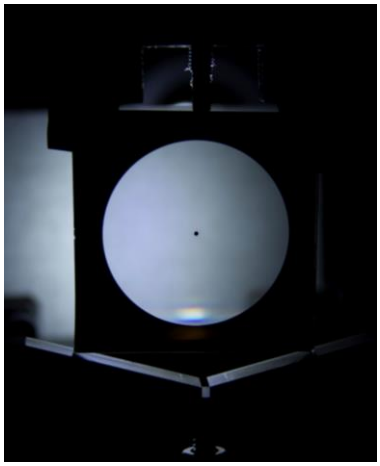

Figure 6. Optical Sieve fabricated at LaRC

The optical sieve fabricated for a telescope for a Heliophysics mission is shown in Figure 6. The aperture size is 2.5 inches with a focal length of 500 mm. The telescope shown in figure was used an H-alpha filter (656.28 nm) with a bandwidth less than 0.5 Angstroms. The bandwidth of the H-alpha filter is much narrower than the bandpass of the optical sieve. Hence, the entire H-alpha line will be in focus. The optical sieve has a point spread function with Strehl ratio of 0.82. Hence the imagery of a USAF bar chart shown in Figure 7 has diffraction limited performance.

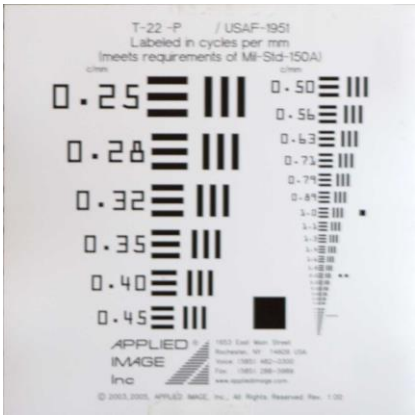

Figure 7. Image of a USAF tri- bar test pattern produced by our diffractive telescope system.

ADAPTIVE OPTICS/BEAM STEERING

Until recently, the phrase adaptive optics generally conjured images of large deformable mirrors being integrated into telescopes to compensate for atmospheric turbulence. However, the development of smaller, cheaper devices has sparked interest for other aerospace and commercial applications. Variable focal length lenses, liquid crystal spatial light modulators, tunable filters, phase compensators, polarization compensation, and deformable mirrors are becoming increasingly useful for other imaging applications including GNC, coronagraphs, foveated imaging, situational awareness, autonomous rendezvous and docking, non-mechanical zoom, phase diversity, and enhanced multi-spectral imaging. The active components presented in this section allow flexibility in the optical design, increasing performance. In addition to performance, adaptive optics technologies offer advantages in size and weight and radiation tolerance making them useful for many small satellite systems.

Referring to the telescope system in Figure 1, the adaptive optics and beam steering can be accomplished by a phase shifting spatial light modulator. A fabricated

liquid crystal polymer on silicon phase shifting array shown in Figure 8. The LCOS device is a 1024x768 pixelated device. Table 2 lists the performance specifications of the LCOS device. The device acts as a deformable mirror device because the backplane is aluminum coated silicon. The front plane is glass. Commercially available off-the-shelf glass is particularly susceptible to radiation-induced coloration due to its amorphous non-crystalline structure[7]. For the LCOS device shown in Figure 8 BK7 glass was used because it has a good CTE (Coefficient of Thermal Expansion) and radiation tolerance[7]. Other transmissive materials which have much higher radiation tolerance, such as BK7G18, LF5G19, can be used. BK7G18 and LF5G19 are stabilized against transmittance loss caused by ionizing radiation by adding cerium to the composition. However, the added cesium does shift the UV transmittance edge to a slightly longer wavelength. Since the front glass is very thin, for most applications (not in the UV) the transmittance loss is very small[7].

Under the metalized back plane are the CMOS electronics that have all the addressing, amplifier and control electronics needed to address each pixel. CMOS micro-electronics are well known to be quite radiation tolerant.

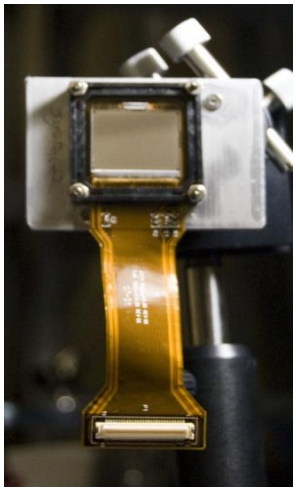

Figure 8. LCOS array of phase shifters

LCOS Performance Evaluation

The Strehl ratio is a useful metric to characterize the compensation performance. Figure 9 shows an uncompensated and compensated beam on the left and right of the figure, respectively. The Strehl ratio, is defined as the normalized peak intensity to diffraction focus. The Strehl ratio of the compensated beam is shown in figure 10. The Strehl ratio was about 100 times higher than the non-compensated beam. Ideally a diffraction limited compensation would yield a Strehl ratio larger than 0.84. One of the main reasons the LCOS is not quite diffraction limited was because the aluminum mirror on the panel did not have a dielectric coating which resulted in a low reflectivity of 80.4%. Note that the Strehl ratio is normalized to the total energy to measure the percent energy contained in the Airy pattern[8]. The beam waist after beam expansion was 9.27 mm, compared with the 20 x 15 mm aperture of the LCOS device. The long axis of the LCOS device is always defined as the Y axis and the short axis is defined as the X axis. The beam waist after beam expansion was 9.27 mm, which means the entire beam is contained within the aperture of the LCOS device of 20 x 15mm. The long axis of the LCOS device is always defined as the Y axis and the short axis is defined as the X axis.

Table 2. Liquid Crystal Polymer on Silicon

Cell Type	Electronic controlled Phase Shifter
Active Area	20 mm x 15mm
Resolution	1024x768
Fill Factor	96.0%
Bit Depth	8 bit (256 gray scale)
Temporal Bandwidth	60 Hz
Effective Stroke Length	635nm
Liquid Crystal Layer Uniformity	1/10 lambda Peak to Valley at 632.8 nm
Operation Wavelength	632.8nm
Beam Steering Range	+/- 4 mrad on both X and Y axis Steering Efficiency > 80.3%
Steering Accuracy	Better than 10 μrad

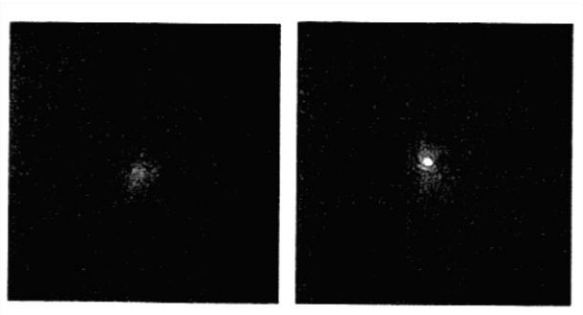

Figure 9. Compensated Beam using a LCOS device

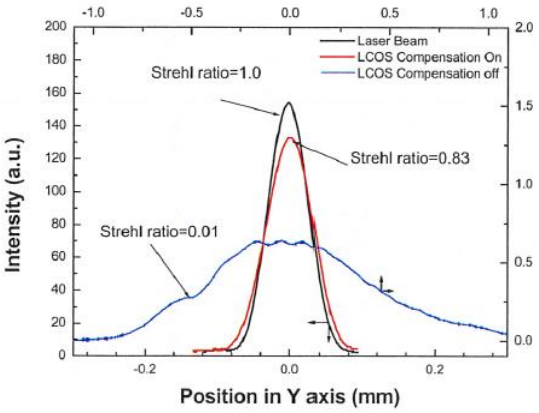

Figure 10. Beam profile of a focused laser beam.

TUNABLE FILTERS

Spectrally tunable filters play a useful role in advanced optical systems. Referring to the diffractive telescope system shown in Figure 1, the tunable filter is useful in controlling the bandwidth so that the entire spectrum passed by the spectral filter is in focus at the focal plane. The spectral filter can also be of very narrow bandwidth to provide hyper-spectral imagery. The LaRC optics fabrication facility provides the means of fabricating a wide range of tunable optical filters tailored for a specific application. One category of tunable filters uses fixed parallel plates filled with a variable refractive index material. When a voltage is applied across these plates the refractive index of the intervening layer changes. A schematic of a 3 stage Lyot and 4 stage solc filter is shown in Figure 10. The Design and performance of such device is described in more detail the literature[9-11].
Another type of tunable filter presented is a Fabry-Perot cavity made with a specially coated elastomeric material, which may have several advantages over the more traditional piezoelectric controlled variety. Archetypal piezo actuated Fabry-Perot filters have employed silicon MOEMS technologies to control the separation between the plates. This implementation may have difficulty maintaining the necessary tight tolerance on the parallel orientation of the plates without complex driving schemes. Furthermore, the

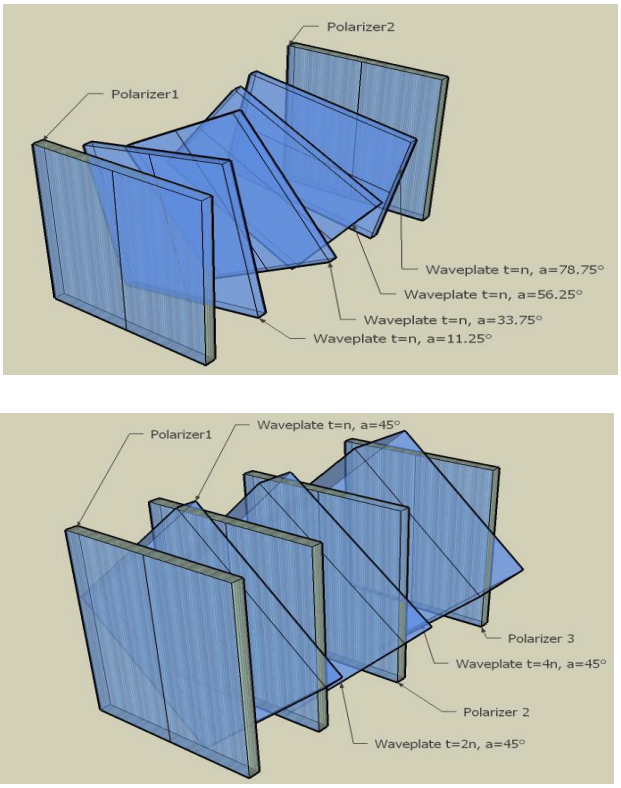

Figure 11. The Lyot spectral filter (top) and Solc spectral filter (bottom).

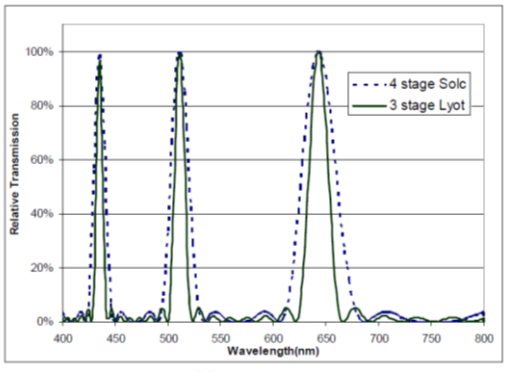

Figure 12. Transmissions of the Lyot and Solc spectral filters.

voltage and thermal requirements of the piezo-electric devices impose difficult and labor-intensive manufacturing and assembly operations, adding cost to the devices and making them less reliable. Langley's compliant polymer based Fabry-Perot etalons offer the advantage of being able to be controlled with lower voltages and over a wider temperature range making them more suited for space exploration applications.

A new breed of MOEMS (Micro Optical Electro Mechanical Systems) devices for space applications are being developed using components made with highly compliant polymeric materials as a principal design element. Typically in MOEMS devices, electrostatic or piezo forces are used to bend or deflect one of the MOEMS layers to produce the desired mechanical motion. Stiffer materials require higher voltages to achieve a given mechanical deflection, and traditional silicon-based materials are all extraordinarily stiff[9].

The Compliant MOEMS technology platform differs from conventional MOEMS by adding a set of softer, more yielding, polymeric materials to the list of conventional rigid silicon-based materials used in MOEMS. Adding these supple materials to the list of materials that can be deposited, patterned and etched greatly widens the design space. The compliant materials used in this new class of MOEMS devices are as much as six orders of magnitude less stiff and can

easily be tailored over a range of three orders of magnitude. Additionally, they can be deposited in a much broader range of layer thicknesses. This very wide range of flexibility expands the design space for MEMS devices far beyond what is possible with traditional silicon-based materials. A Fabry-Perot is an optically resonant cavity formed by two highly-parallel, partially transparent mirrors. The separation of the mirrors and optical path length of the round trip can be used to control the transmission spectrum. To the first order, we can use the Airy formula given below to estimate this spectrum[9].

$$T(\lambda, L) = \frac{1}{1+\frac{4R}{(1-R)^2}(\sin\left(\frac{2\pi n(\lambda)d}{\lambda}\right))^2} \quad (1)$$

where R is the reflectivity of the windows, d is the separation of the plates, λ is the wavelentth and n(λ) is the index of refraction of the intervening media. In collimated light at normal incidence, the free spectral range (FSR), or wavelength separation of the two neighboring peaks is approximated by:

$$FSR(\lambda, L) = \frac{\lambda^2}{2n(\lambda)d} \quad (2)$$

where the variables are the same as defined above. This also has to do with fringe frequency, and is defined as the separation between adjacent orders of interference. This definition to how far the moving mirror must move to arrive at the next order of the constructive interference which occur every $n\lambda/2$. The process of calibrating and controlling our pixilated Fabry Perot Etalon array is ongoing. Figure 15 shows the spectrum from the Etalon. The mirrors can be driven to L<1 micron. There is currently no insulation layer on the electrode and due to the tile on the mirror it cannot be driven much below 5 microns without shorting the etalon mirrors together. Work is continuing on developing a specialized insulating layer and tilt control mechanism for the Etalon array

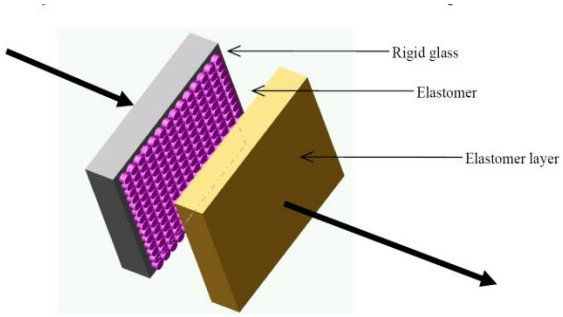

Figure 13. Schematic of a Elastomer Fabry Perot Etalon Array.

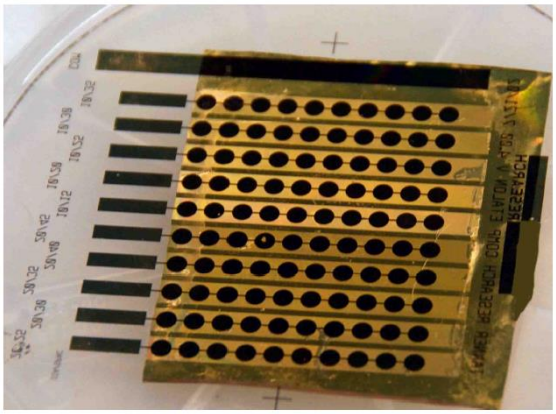

Figure 14 16 x 16 Array of Elastomer Fabry Perot Etalons.

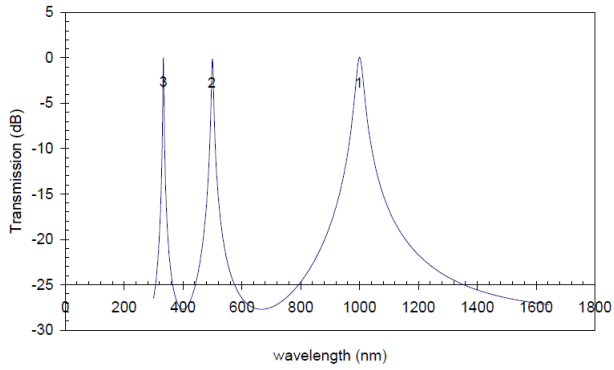

Figure 15. Spectral Transmission of Fabry Perot Etalons.

INERTIAL MEARUREMENT UNIT

An auto correcting inertial measurement unit (IMU) is also being developed by integrating three evolving and innovative technologies. These technologies include (1) the LaRC intelligent star tracker[12-13] (2) a high precision high bandwidth inertial rate sensor and (3) and advance sensor fusion algorithm based on the extended Kalman filter.

The LaRC star tracker system was developed under DARPA, NASA NRA, and AFOSR programs. The resulting Star tracking system is shown in Figure 16. Conventional star tracker system use all glass components for a wide field of view. The LaRC star tracker system uses a folded telescope to reduce the weight to under 0.75 Kg. Telescopes inherently have a narrow field of view of typically 0.1 degrees. To enable the star tracker system to have a large field of view, a specially designed corrector plate enables the star sensor to achieve a 20 degree field of view. The corrector place also corrects for optical aberrations of the star tracker system to optimize for tracking accuracy. The star tracker specs are shown in Table 3. The inertial sensor has a 1 kHz bandwidth and accuracy of 50 nano-radians.

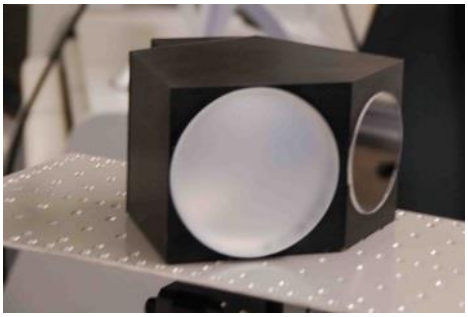

Figure 16. LaRC Intellistar star tracker system.

Table 3. LaRC Intellistar Star Tracker System

Sensitivity	**+1 to +6**
Aperture	**68 mm**
Weight	**.75 kg**
Number of stars tracked	**1 to 5**
Angular accuracy	**7 micro- radians**
FOV	**20 degrees (full frame sensor)**
Update rate	**10 Hz**
Output	**Quaterion**

SUMMARY

Optical imaging is important for many NASA missions. The size, weight, and cost of optical components increase exponentially with aperture size. For low light and high resolution imaging large aperture telescopes are usually required. Synthesized nano-layered materials enable materials t be combined using nano photonics fabrications significant reduction in in weight and cost. Most importantly, NASA science missions including Heliophysics, exoplanet, optical communications and GNC applications require some of the most demanding optical performance metrics. Hence, the nano-layered synthesized materials are key to enabling small satellite systems to have high performance.

REFERENCES

1. Yeh, Pochi, "Optical waves in layered media", John Wiley & Sons, March 2005

2 Hickey, Greg; Lih Shyh-shiuh et al, " Development of Nanolaminate thin shell mirrors, *SPIE* 4849, Highly Innovative Space Telescope Concepts, 63 (December 1, 2002)

3. Xie, Shixang, Zhang, Zhijian and Wei,Wei " Synthesis and properties of Polyimide based optical materials", Journal of the Korean Physical Society, Vol 51 No. 4, October 2007, pp. 1536-1541

4. L. Kipp, M. Skibowski, R. L. Johnson, R. Berndt, R. Adelung, S. Harm, and R. Seemann, Sharper images by focusing soft xrays with photon seives, Nature 414, 184 (2001)

5. Rajesh, Menon and Dario, Gil, "Photon-sieve lithography", J. Opt Soc Am. A/Vol22, No. 2 February 2005.

6. Andersen, Geoff "large optical photon sieve", Optics Letters Vol 30 No 22. November 2005.

7 Schott Glass, TIE-42: Radiation Resistant Optical Glasses, August 2007

8. Robert K Tyson "Principles of Adaptive Optics", Academic Press; 2 edition (October 13, 1997).

9. Crandall C, Clark N., Davis P. "Tunable optical filters for space exploration", SPIE 6713 Nanophotonics and Macrophotonics for Space Environments, September 2007 pp

10. I. Solc, "Birefringent Chain Filters," Journal of the Optical Society of America, **55**, 621 (1965).

11. H. Wright, C. Crandall & P. Miller, Active filters enable color imaging, Laser Focus World, May 1996.

12. Clark N. "Design and performance evaluation of sensors and actuators for advance optical systems", in Nanosensors, Biosensors, and Info-Tech Sensors and Systems 2011, Vijay K. Varadan, Editors, Proceedings of SPIE Vol. 7980 (SPIE, Bellingham, WA 2011), 798004.

13. Clark N. "Intelligent star tracker", in Device and Process Technologies for MEMS and Microelectronics II, Jung-Chih Chiao; Lorenzo Faraone; H. Barry Harrison; Andrei M. Shkel, Editors, Proceedings of SPIE Vol. 4592 (SPIE, Bellingham, WA 2001), pp.216-226.